Inorg. Chem. **2007**, *46*, 1535–1537

Resolution of Enantiomers in Solution and Determination of the Chirality of Extended Metal Atom Chains

Daniel W. Armstrong,*,† F. Albert Cotton,*,‡ Ana G. Petrovic,§ Prasad L. Polavarapu,*,§ and Molly M. Warnke†

Department of Chemistry and Biochemistry, University of Texas at Arlington, Arlington, Texas 76019, Department of Chemistry and Laboratory for Molecular Structure and Bonding, P.O. Box 30012, Texas A&M University, College Station, Texas 77842-3012, and Department of Chemistry, Vanderbilt University, Nashville, Tennessee 37235

Received November 28, 2006

The resolution of enantiomers of extended metal atom chains of the type $Ni_3[(C_5H_5N)_2N]_4Cl_2$ has been accomplished by chromatographic methods in solution, and the chirality was determined using vibrational circular dichroism, electronic circular dichroism, optical rotatory dispersion, and density functional theory calculations.

Among the multifarious approaches[1,2] to making molecular wires is one that aims to take the image of a real-life wire and scale it down to the greatest possible extent, as shown in Figure 1. Most efforts to follow this particular approach have entailed the use of poly(pyridylamide) ligands (Chart 1). In this way, the metals Cr ($n = 0-2$), Co ($n = 0-2$), Ni ($n = 0-3$), Cu ($n = 0$), Ru ($n = 0$), and Rh ($n = 0$) have been incorporated into molecules of the type shown in Figure 2 for the case of $n = 0$, and some of their properties (especially) for $n = 0$ have been studied in detail.[2] For $n = 0$, the anion, dpa, is derived from dipyridylamine. One of the intrinsic properties of the chirality of extended metal atom chains (EMACs) is that they have a helical winding of the four insulating polypyridyl ligands around the central metal *wire*, but these species are typically isolated as racemic crystals. In one case where chiral crystals are formed, $[Co_3(dpa)_4(CH_3CN)_2](PF_6)_2$,[3] the enantiomorphous crystals had to be separated by hand. To determine whether the conformation was *P* or *M*[4] (Chart 2), each crystal had to be examined by X-ray crystallography. A general, simple approach for resolving chiral EMAC-type molecular wires, and establishing their chirality, is presented here for the first time.

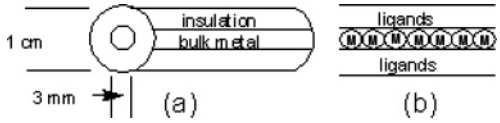

Figure 1. How a normal wire (a) may be reduced to the smallest possible molecular wire (b).

Chart 1. Poly(pyridylamide) Ligands

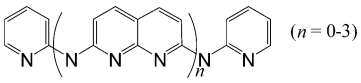

The results given here are for $Ni_3(dpa)_4XCl$ molecules, where X represents Cl (**1a**) or OH (**1b**). Extensive efforts to obtain single crystals of the individual enantiomers were unsuccessful, but a few racemic crystals that appeared because of incomplete separation revealed that there was a roughly 1:1 mixture of Cl^- and OH^- axial anions. The replacement of Cl by OH evidently occurs in the course of the chromatographic separation. The separation of the *P* and *M* isomers was achieved by use of a preparative chromatographic procedure using a macrocyclic glycopeptide-based chiral stationary phase.[5,6]

After collection of each enantiomer as it eluted from the column, the solvent from each enantiomeric mixture was evaporated to dryness. The samples were then dissolved in dichloromethane and washed with deionized water to remove the salt that was left from the mobile phase. The desiccant

* To whom correspondence should be addressed. E-mail: sec4dwa@uta.edu (D.W.A.), cotton@tamu.edu (F.A.C.), Prasad.L.Polavarapu@vanderbilt.edu (P.L.P.).
† University of Texas at Arlington.
‡ Texas A&M University.
§ Vanderbilt University.

(1) In *Extended Linear Chain Compounds*; Miller, J. S., Ed.; Plenum Press: New York, 1982.
(2) (a) Cotton, F. A.; Murillo, C. A. *Eur. J. Inorg. Chem.* **2006**, *21*, 4209. (b) Berry, J. F. Extended Metal Atom Chains. In *Multiple Bonds Between Metal Atoms*; Cotton, F. A., Murillo, C. A., Walton, R. A., Eds.; Springer Science and Business Media, Inc.: New York, 2005; pp 669−706. (c) Chae, D.-H.; Berry, J. F.; Jung, S.; Cotton, F. A.; Murillo, C. A.; Yao, Z. *Nano Lett.* **2006**, *6*, 165. (d) Berry, J. F.; Cotton, F. A.; Lu, T.; Murillo, C. A.; Wang, X. *Inorg. Chem.* **2003**, *42*, 3595.
(3) Clérac, R.; Cotton, F. A.; Dunbar, K. R.; Lu, T.; Murillo, C. A.; Wang, X. *Inorg. Chem.* **2000**, *39*, 3065.
(4) In a helical system, *P* and *M* stand for positive or negative as they relate to the torsion angles along the axis of the helix. For example, see: (a) Nasipuri, D. *Stereochemistry of Organic Compounds*; Wiley Eastern Ltd.: New Delhi, India, 1991. (b) Cahn, R. S.; Ingold, C.; Prelog, V. *Angew. Chem., Int. Ed. Engl.* **1966**, *5*, 385. (c) Taber, D. F.; Malcolm. S. C.; Bieger, K.; Lahuerta, P.; Sanaú, M.; Stiriba, S.-E.; Pérez-Prieto, J.; Monge, M. A. *J. Am. Chem. Soc.* **1999**, *121*, 860.

10.1021/ic062263l CCC: $37.00
Published on Web 02/02/2007

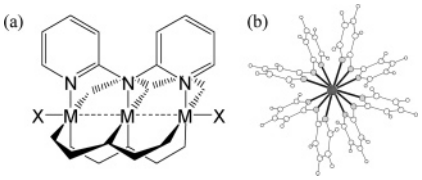

Figure 2. (a) Schematic drawing of an $M_3(dpa)_4X_2$ EMAC. (b) End view showing the helicity (*P* in this case).

Chart 2. Representation of the *P* helicity of Dipyridyl Ligands

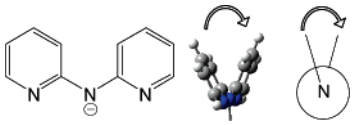

sodium sulfate was added to each of the enantiomer/dichloromethane mixtures and then allowed to stand for several hours to remove excess water. The sodium sulfate was then removed, and the dichloromethane was evaporated, leaving the resolved EMAC enantiomers.

To determine the absolute configuration of each enantiomer, chiroptical spectroscopic techniques were utilized. These included[7] vibrational circular dichroism (VCD), electronic circular dichroism (ECD), and optical rotatory dispersion (ORD). The final interpretation was assisted by density functional theory (DFT) calculations. In this report, the labels $(+)_{589nm}$ and $(-)_{589nm}$ are employed to designate the signs of optical rotation (OR) of the enantiomers at 589 nm.

The vibrational absorbance (VA) and VCD spectra of $(+)_{589nm}$-**1** and $(-)_{589nm}$-**1** were recorded in the mid-IR spectral region, from 2000 to 900 cm^{-1}, with a 1 h data collection time, at 8 cm^{-1} resolution.[8] In the absorption and VCD spectra, shown in Figure 3, the solvent spectra were subtracted to establish the zero baseline. Additionally, a small

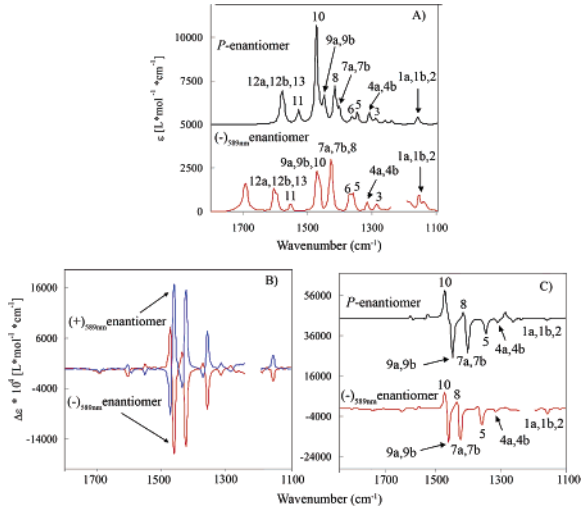

Figure 3. VA (panel A) and VCD spectra of **1**. The experimental VCD spectra are shown for both enantiomers in panel B. Calculated spectra for *P*-**1a** (topmost trace in panels A and C) were obtained with B3LYP/LANL2DZ. Calculated spectra in panels A and C have been shifted up for clarity.

frequency region between ~1238 and 1196 cm^{-1} has been excluded because the presence of a strong solvent absorption band in this region makes the solvent subtraction difficult.

OR as a function of the concentration was measured on an Autopol IV polarimeter, using a 1.0 dm cell. Solutions of $(+)_{589nm}$- and $(-)_{589nm}$-**1** in a $CHCl_3$ solvent were prepared by successive dilutions from a parent stock solution. OR measurements were made at all wavelengths accessible by the polarimeter: 633, 589, 546, 436, 405, and 365 nm. These concentration-dependent studies have resulted in data points ranging in concentration from ~0.00013 to 0.000013 g/mL for the $(-)_{589nm}$ enantiomer and from ~0.000181 to 0.0000181 g/mL for the $(+)_{589nm}$ enantiomer. The intrinsic rotation, which represents specific rotation at infinite dilution, was extracted from the ORs at different concentrations.

The calculations of vibrational frequencies, IR absorptions, VCD, and ECD were performed with the *Gaussian 03* program.[9] Geometry optimization was first carried out with the B3LYP functional. The same functional was also used for the VA and VCD calculations. On the basis of previous experience,[10] the BHLYP functional, which uses an increased admixture of Hartree−Fock exchange in time-dependent DFT calculations, was also employed. The LANL2DZ basis set[11] was used for all computations. A Kramers−Kronig transform of the calculated ECD intensities provided the ORD spectrum.[12] The theoretical absorption and VCD spectra were simulated with Lorentzian band shapes and a 5 cm^{-1} half-width at half-peak height. The calculated vibrational frequencies have been scaled by a factor of 0.9612. The theoretical ECD spectrum was simulated from the first 50 singlet → singlet electronic transitions using Gaussian band shapes and a 20 nm half-width at 1/*e* of peak height.

(5) A semipreparative (250 × 21.2 mm) Chirobiotic V macrocyclic glycopeptide-based chiral stationary phase was used. The stationary phase was obtained from Advanced Separation Technologies (Whippany, NJ). The mobile phase consisted of 95/5/0.15 ACN/MeOH/NH_4-TFA pumped at a flow rate of 8 mL/min. The trinickel dipyridylamido complex was dissolved in 60/40 ACN/MeOH before injection. A high-performance liquid chromatography (HPLC) system consisting of a pump (LC-6A; Shimadzu, Kyoto, Japan), a system controller (SCL-6A), Chromatopac (CR 601; Shimadzu), a UV detector (SPD-6A; Shimadzu), and a 200 μL injector valve (Rheodyne, Cotati, CA) was used. The wavelength of detection was 270 nm. Chiral detection was performed with a Jasco CD-2095 (Easton, MD) circular dichroism detector. See: Warnke, M. M.; Cotton, F. A.; Armstrong, D. W. *Chirality* **2007**, *19*, 179.

(6) For the chromatographic procedure, the methanol (MeOH) and acetonitrile (ACN) used in the mobile phases are HPLC grade and were purchased from VWR (West Chester, PA) as well as the dichloromethane used in extraction. Ammonium trifluoroacetate (NH_4TFA) was purchased from Aldrich (Deerfield, IL) and sodium sulfate was purchased from Fisher (Fair Lawn, NJ). HPLC-grade water from an in-house Milli-Q system was used for extractions. Mobile phases were degassed with helium for 5 min.

(7) For recent reviews in VCD, ECD, and ORD, see: (a) Polavarapu, P. L.; He, J. *Anal. Chem.* **2004**, *76*, 61A. Freedman, T. B.; Cao, X.; Dukor, R. K.; Nafie, L. A. *Chirality* **2003**, *15*, 743. Stephens, P. J.; Devlin, F. J. *Chirality* **2000**, *12*, 172. (b) Pecul, M.; Ruud, K.; Helgaker, T. *Chem. Phys. Lett.* **2004**, *388*, 110. Diedrich, C.; Grimme, S. *J. Phys. Chem. A* **2003**, *107*, 2524. (c) Polavarapu, P. L. *Chirality* **2006**, *18*, 348. Crawford, T. D. *Theor. Chem. Acc.* **2006**, *115*, 227.

(8) Spectra were measured in a demountable cell containing CaF_2 windows and a 200 μm path length spacer and at a concentration of ~0.0126 M in a $CHCl_3$ solvent environment using a commercial Fourier transform VCD spectrometer, Chiralir.

(9) *Gaussian 03*; Gaussian Inc.: Wallingford, CT.

(10) Polavarapu, P. L.; He, J.; Crassous, J.; Ruud, K. *ChemPhysChem* **2005**, *6*, 2535.

(11) Hay, P. J.; Wadt, W. R. *J. Chem. Phys.* **1985**, *82*, 270.

(12) Polavarapu, P. L. *J. Phys. Chem. A* **2005**, *109*, 7013.

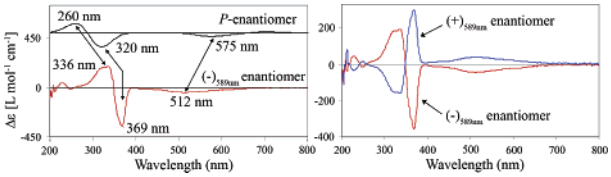

Figure 4. Electronic CD spectra of **1**. Experimental ECD spectra are shown for both enantiomers in the right panel. The predicted spectrum for *P*-**1a** (topmost trace in the left panel) was obtained with time-dependent BHLYP/LANL2DZ and shifted up for clarity.

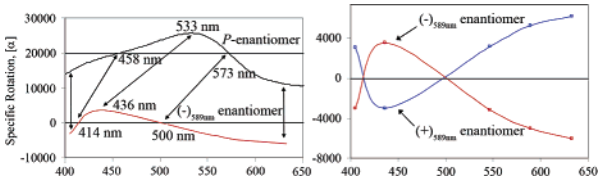

Figure 5. ORD spectra of **1**. The right panel shows experimental spectra for the two enantiomers, while the left panel shows a comparison between the predicted ORD for the *P* enantiomer of **1** and the experimental spectrum for the $(-)_{589nm}$ enantiomer of **1**.

Panel A in Figure 3 shows the observed VA spectrum from 1100 to 1750 cm^{-1} and the calculated spectrum for the *P* enantiomer. The absorption bands are labeled, and a key to the assignments is provided as Supporting Information. The computation was done for **1a**, and no account was taken of the fact that some axial OH groups were present in the experimental sample. This is why the Ni−O−H bending mode at ca. 1700 cm^{-1} is not in the computed spectrum. The ∼1190−1240 cm^{-1} gap corresponds to strong absorption interference from the $CHCl_3$ solvent. Panel B of Figure 3 shows the mirror-image VCD spectra of the $(+)_{589nm}$ and $(-)_{589nm}$ enantiomers. In panel C, the VCD spectrum of the $(-)_{589nm}$ enantiomer is compared with the VCD spectrum calculated for the *P* enantiomer.

The mirror-image ECD spectra[13] of the $(+)_{589nm}$ and $(-)_{589nm}$ enantiomers of **1b** and their comparison to the predicted ECD spectrum for the *P* enantiomers are shown in Figure 4. It is clear that the $(-)_{589nm}$ enantiomer has *P* helicity, in agreement with the conclusion from the VCD results. The experimental ORD spectrum in the 400−650 nm region for the $(-)_{589nm}$ enantiomer shown in Figure 5 exhibits a negative−positive−negative feature, which is reproduced by the ORD predicted for the *P*-helical structure. As for the ECD, the predicted positive ORD maximum at 533 nm and zero crossing positions at 458 and 573 nm are shifted from the corresponding positions (436, 414, and 500 nm, respectively) in the experimental ORD. These shifts are not unusual because it is well-known[14] that DFT calculations do not yield accurate wavelengths for the electronic transitions.

The agreement between the theoretical and experimental chiroptical spectra (VCD, ECD, and ORD) leads to the conclusion that the $(-)_{589nm}$ enantiomer of **1** has the *P*-helical configuration and, conversely, the $(+)_{589nm}$ enantiomer of **1** has the *M*-helical configuration.

Acknowledgment. We thank Dr. John F. Berry for supplying the racemic nickel compound. Support from the NSF, the Robert A. Welch Foundation (to D.W.A. and F.A.C.), and the Texas A&M University (to F.A.C.) is gratefully acknowledged. A grant from the National Computational Science Alliance (to P.L.P.; Grant CHE040009N) supported the computational work utilizing the IBM P690 at the University of Illinois. A teaching assistantship (to A.G.P.) from Vanderbilt University is gratefully acknowledged. D.W.A. and M.M.W. also acknowledge the support of the National Institutes of Health (NIH R01 GM53825-11).

Supporting Information Available: Tables of Cartesian coordinates, VCD and ECD intensities, and vibrational frequency assignments, the structure and a chromatogram of enantioseparation for $Ni_3(dpa)_4Cl_2$, and the full citation for ref 9. This material is available free of charge via the Internet at http://pubs.acs.org.

IC062263L

(13) The ECD spectra were recorded on a Jasco J720 spectrometer in the 200−800 nm region, using a 0.01 cm path length cell. The concentration was ∼0.00129 M in a $CHCl_3$ solvent.

(14) Bauernschmitt, R.; Ahlrichs, R. *Chem. Phys. Lett.* **1996**, *256*, 454.